

Species-selective microwave cooling of a mixture of rubidium and caesium atoms

This article has been downloaded from IOPscience. Please scroll down to see the full text article.

2007 New J. Phys. 9 147

(<http://iopscience.iop.org/1367-2630/9/5/147>)

View [the table of contents for this issue](#), or go to the [journal homepage](#) for more

Download details:

IP Address: 131.220.157.241

The article was downloaded on 23/11/2010 at 10:51

Please note that [terms and conditions apply](#).

Species-selective microwave cooling of a mixture of rubidium and caesium atoms

M Haas, V Leung¹, D Frese, D Haubrich, S John, C Weber,
A Rauschenbeutel² and D Meschede³

Institut für Angewandte Physik, Universität Bonn, Wegelerstraße 8,
53115 Bonn, Germany

E-mail: meschede@uni-bonn.de

New Journal of Physics **9** (2007) 147

Received 7 February 2007

Published 23 May 2007

Online at <http://www.njp.org/>

doi:10.1088/1367-2630/9/5/147

Abstract. We have sympathetically cooled a small sample of ^{133}Cs atoms with ^{87}Rb to below $1\ \mu\text{K}$. Evaporative cooling was realized with microwave radiation driving the Rb ground-state hyperfine transition. By analysing the sympathetic cooling dynamics, we derive a lower limit of the modulus of the Rb–Cs interspecies triplet s -wave scattering length of $200\ a_0$. For temperatures below $5\ \mu\text{K}$ we observe strong non-exponential losses of the Cs sample in the presence of the Rb sample.

Contents

1. Introduction	2
2. Rb–Cs mixtures	2
3. Experimental set-up	3
4. Experiments and results	4
5. Conclusions and outlook	9
Acknowledgments	9
References	9

¹ Present address: Groupe d'Optique Atomique, Laboratoire Charles Fabry, Institut d'Optique, Bâtiment 503, 91403 Orsay, France

² Present address: Institut für Physik, Johannes Gutenberg-Universität, Staudingerweg 7, D-55128 Mainz, Germany

³ Author to whom any correspondence should be addressed.

1. Introduction

Since the realization of Bose–Einstein condensation (BEC), quantum degenerate atomic gases have become important and widespread in many laboratories for studies of many-particle phenomena at ultralow temperatures and in the quantum limit. Two-component mixtures of ultracold atomic ensembles offer additional degrees of freedom beyond homogeneous systems: the interacting system can not only be studied in its own right, a single species can also be used as an agent to control the whole system. Sympathetic cooling is a well-known example where one species cooled directly by, e.g. evaporative cooling, indirectly cools the other one through collisional interactions. For instance, with sympathetic cooling the suppression of *s*-wave collisions in fermionic atomic quantum gases was circumvented and led to the breakthrough of reaching quantum degeneracy in such systems [1, 2]. Binary mixtures of ultracold gases have further interesting prospects. This includes the formation of heteronuclear molecules, which requires mixtures of ultracold atomic gases. Production of ultracold KRb [3], $^{85}\text{Rb}^{87}\text{Rb}$ [4] and RbCs [5] molecules has been demonstrated already. An interesting application as molecular qubits has been proposed for stored polar RbCs molecules by DeMille [6]. Recently there has been growing interest in the combination of single atom physics with ultracold quantum gases. Experiments with a small number of quantum-correlated atoms promise to shed new light onto the transition from single particles to the world of correlated many-particle systems. For instance, exactly known numbers of quantum-degenerate bosonic atoms in their motional ground-state were prepared [7]. In the case of a very small number (atom number $N < 10$) of dopants inside a Bose–Einstein host condensate, theoretical studies predict impurity–impurity interactions mediated by the condensate [8]. The control of the state of the entire condensate by manipulation of an individual impurity has been proposed [9]. Another interesting prediction is the possibility to cool single atoms to their motional ground-state while preserving their coherent state [10].

To date, two-species experiments have worked with large samples ($N \geq 10^4$) of atoms of each species and most of them with a comparable atom number for both species [11]–[13]. We plan to combine the physics of single atoms and ultracold quantum gases by experimentally realizing quantum degenerate mixtures of atomic gases where one component is rarified to the level of 1–100 atoms only. Extending the proposals mentioned above one could address more general physical questions concerning the way in which many-particle concepts are reflected at the level of very small samples of atoms. Furthermore one could study the possibility of using Bose condensates to control the properties of a small number of impurity atoms. And eventually one could explore the feasibility of the deterministic creation of a single heteronuclear molecule. In all cases of interest tight experimental control, i.e. ultralow temperatures as well as tunable interactions between atoms of the two species of the mixture will be essential.

2. Rb–Cs mixtures

A mixture of Rb and Cs seems attractive for the preparation of very small samples of ultracold atoms: (i) BECs of ^{87}Rb can be prepared with relative ease to act as refrigerators for a small number of ultracold Cs atoms; (ii) sympathetic cooling in magnetic traps is favoured by the similar ratio of magnetic moment to mass for Rb and Cs atoms; (iii) both Rb and Cs have a large polarizability, suggesting a strong interaction; (iv) nearly all experiments with single neutral atoms use Rb or Cs. In addition, the RbCs molecule is very polar [5], making it an interesting

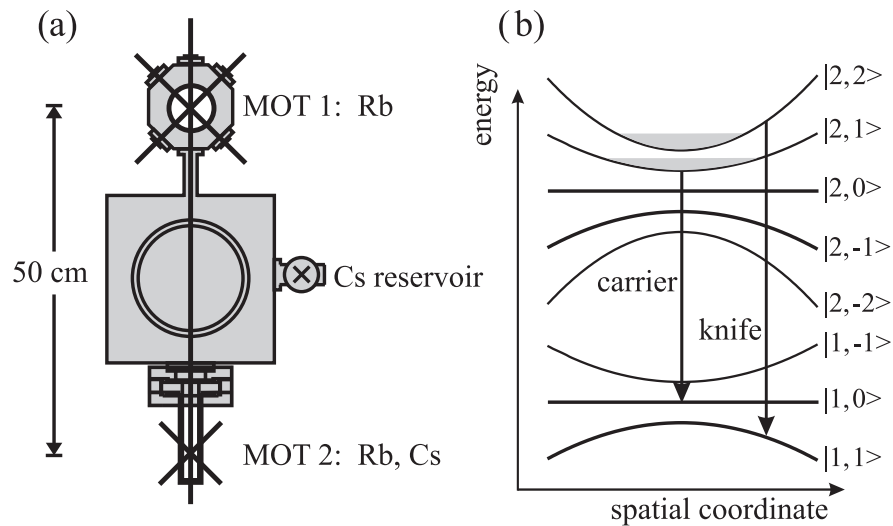


Figure 1. (a) Schematic of the experimental apparatus showing the vacuum set-up, the Rb-double-MOT system including the laser beam transferring Rb from MOT 1 to MOT 2, the Cs-MOT and the Cs reservoir in the ultra high vacuum (UHV) region. (b) Microwave induced transitions in Rb. The carrier is fixed in frequency while the frequency of the knife is lowered continuously.

candidate to serve as a qubit in quantum information processing [6]. One may even envision trying to produce small known numbers of RbCs molecules in a controlled way.

As of now, the knowledge about the Rb–Cs interaction potentials is not sufficient to make precise predictions on the interaction strength, or the location of interspecies Feshbach resonances [14]. A first experiment to measure the triplet *s*-wave scattering length in the Rb–Cs system was carried out at the University of Pisa with rethermalization measurements [15, 16] for different mean temperatures of the mixture. By comparing the experimental results with the theoretical predictions from [14] the authors assigned the triplet *s*-wave scattering length a value of $595 a_0$, where a_0 is the Bohr radius and no uncertainty was given.

In this work, we report on studies with mixtures of ^{87}Rb and ^{133}Cs trapped in a magnetic trap. We demonstrate sympathetic cooling of Cs down to temperatures below $1 \mu\text{K}$. Rb is cooled by microwave evaporative cooling [17] on the 6.8 GHz ground state hyperfine transition. Due to the large difference in the hyperfine splittings of Rb and Cs ($\approx 9.2 \text{ GHz}$) this cooling method is species-selective and avoids any evaporative losses of Cs during the cooling process. From our sympathetic cooling measurements we can derive a lower limit for the modulus of the triplet *s*-wave scattering length. The relative atom numbers can be chosen such that $N_{\text{Cs}}/N_{\text{Rb}} \ll 1$, in preparation for future experiments within the regime outlined above. One important initial task is the determination of collisional properties in the Rb–Cs system.

3. Experimental set-up

We produce the ultracold Rb–Cs mixtures in an experimental set-up based on a double-MOT (magneto-optical trap) BEC apparatus: a small vacuum chamber, where the Rb atoms are collected in a vapor pressure MOT, and—connected by a differential pumping tube—a large

UHV chamber, to which a glass cell is mounted (see figure 1(a)). Inside the glass cell the second Rb-MOT, the Cs-MOT and the magnetic trap—a quadrupole and Ioffe configuration (QUIC) trap as described in [18]—are located. To realize a two-species MOT in the UHV region the MOT beams for the two species are overlapped with the help of a dichroic mirror. We use a single set of optical components with a broadband near-infrared coating suitable for both wavelengths. This includes high order waveplates used for intensity distribution and the creation of circular polarization of the MOT beams. To optimize the size and the position of the Rb and the Cs MOT independently, additional waveplates are included that act only on the intensity distribution of the trapping light of one species. The Rb atoms are transferred from the vapour pressure MOT to the second MOT by a near resonant laser beam [19] whereas Cs diffuses from a reservoir in the UHV region to the trapping region of the second MOT (see figure 1(a)). The reservoir can be closed by a valve and thereby it is possible to adjust the Cs partial pressure, i.e. the number of Cs atoms captured in the MOT. When this valve is closed the background pressure in the UHV region is $\sim 2 \times 10^{-11}$ mbar. We have found that even after operating at a relatively high pressure of $\sim 10^{-9}$ mbar, we can recover this pressure within a period of several days. In addition we employ light-induced atomic desorption (LIAD) to increase the Cs partial pressure in the MOT region [20]. We use as a light source a powerful UVA LED array from Roithner Lasertechnik; this allows us to capture up to $\sim 10^7$ atoms in the Cs-MOT with a steady-state background pressure of around 2×10^{-10} mbar. Atom numbers and temperatures are extracted by absorption imaging of the atom clouds after a variable time of free expansion. The probe beams for both species are overlapped with a dichroic mirror and pass through the same imaging optics. Before the Rb and Cs atoms are loaded into the magnetic quadrupole trap, they are optically pumped to the states $|F = 2, m_F = 2\rangle$ and $|F = 4, m_F = 4\rangle$ respectively. After adiabatic compression in the quadrupole trap the atoms are transferred to the final QUIC trap configuration. For Rb the radial and axial trap frequencies are $\omega_{\text{rad}} = 2\pi \cdot 189$ Hz and $\omega_{\text{ax}} = 2\pi \cdot 9$ Hz respectively, while those for Cs are a factor of $\sqrt{m_{\text{Rb}}/m_{\text{Cs}}} = 0.81$ smaller. Typical initial conditions in the QUIC trap for Rb are atom numbers of $2\text{--}3 \times 10^8$ and temperatures of $180\text{--}250$ μK . The corresponding values for Cs cannot be measured directly, as the optical density is too small to be accurately determined from absorption images. However, from measurements at higher optical densities obtained by sympathetic cooling we can infer an initial Cs atom number of $\gtrsim 10^6$. Forced evaporative cooling of Rb is performed on the 6.8 GHz ground state hyperfine transition; the corresponding transition frequency in Cs at 9.2 GHz is far-detuned and thus the cooling is species-selective. The microwave source consists of a phase-locked loop coaxial resonator (Model BCO-010-06830-05, manufactured by Miteq), which acts as the local oscillator. Its output frequency can be set within a small interval around 6.83 GHz. Using a standard 1 : 1 mixer the output of the local oscillator is modulated with frequencies in the range from 1–80 MHz. The upper sideband is used for transferring the Rb atoms energy-selectively from the $|2, 2\rangle$ to the non-trapped $|1, 1\rangle$ state. The evaporation ramp is realized by lowering the frequency of the upper sideband in several linear steps and its duration for the measurements presented here is on the order of 20 s. The output of the mixer is amplified by a pre-amplifier and a power amplifier. A simple rectangular waveguide is used as an antenna.

4. Experiments and results

While attempting to evaporatively cool Rb with this method down to quantum degeneracy, we found that the $|2, 1\rangle$ state becomes significantly populated, as shown in figure 2. The atoms in

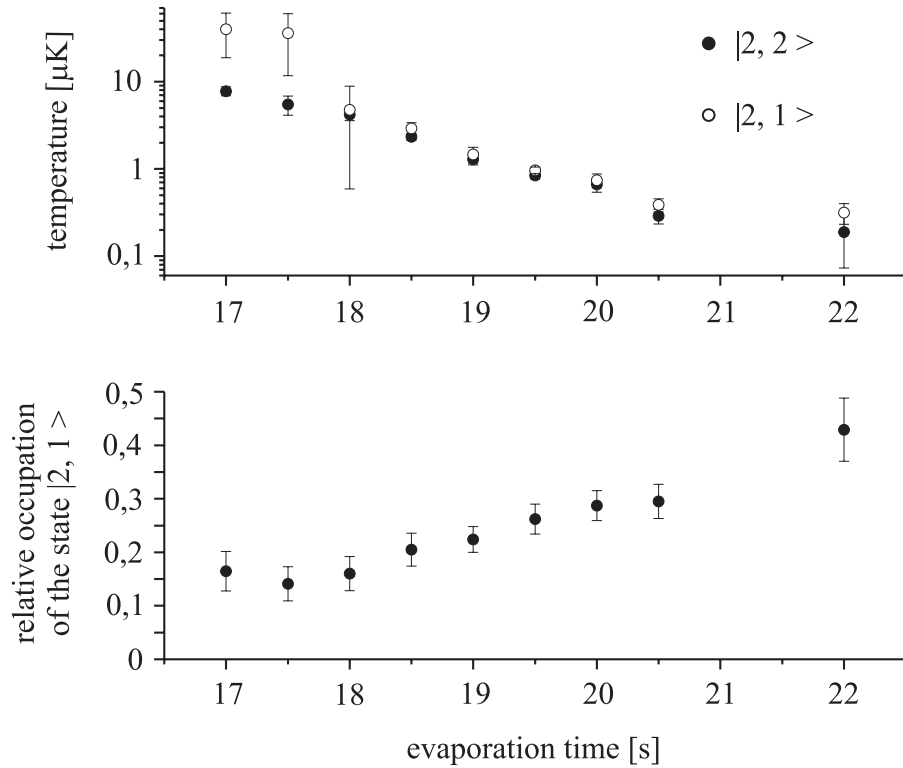


Figure 2. Upper graph: temperature of Rb atoms in the $|2, 2\rangle$ and $|2, 1\rangle$ state respectively. Lower graph: relative population $N_{\text{rel}} = N_{21}/(N_{22} + N_{21})$ of the $|2, 1\rangle$ state of Rb. To separate the two clouds, an inhomogeneous magnetic field was applied after the trap was switched off.

the different m_F states were spatially separated by applying an inhomogeneous magnetic field after the trap was switched off. We performed the following experiment to exclude insufficient optical pumping as the reason for the occupation of the $|2, 1\rangle$ state. Before transferring the atoms to the QUIC trap, the gradient in the magnetic quadrupole trap was ramped down and held for 1 s at a value where Rb in the $|2, 1\rangle$ state cannot be held against gravity. Rb was evaporatively cooled as before and we found that the population of the $|2, 1\rangle$ state was unchanged. We also checked whether the $|2, 1\rangle$ state is populated due to inelastic collisions. To do so, pure $|2, 2\rangle$ samples of $\sim 2\text{--}4 \times 10^6$ atoms were prepared (see below) at temperatures of $1\text{--}2 \mu\text{K}$ and stored for up to 30 s, with the microwave source switched off. After the storage an inhomogeneous magnetic field was applied after trap switch-off but no atoms were found in the $|2, 1\rangle$ state. Therefore we exclude inelastic collisions to be of relevance for the transfer of Rb atoms from the $|2, 2\rangle$ to the $|2, 1\rangle$ state in our system. We suggest that atoms transferred to the $|1, 1\rangle$ state are pumped back to the $|2, 1\rangle$ state after travelling some distance to become again resonant with the microwave radiation. The creation of Rb atoms in the $|2, 1\rangle$ state was also reported in [21], where the same transition was used for the evaporative cooling of Rb and population of the $|2, 1\rangle$ state is attributed to inelastic collisions at a high magnetic bias field [21, 22].

We remove the atoms in the $|2, 1\rangle$ state by choosing the microwave carrier frequency, which is equal to the local oscillator frequency, such that it transfers $|2, 1\rangle$ atoms to the $|1, 0\rangle$ state (see figure 1(b)). Using the same evaporation ramp as for the measurements presented in figure 2

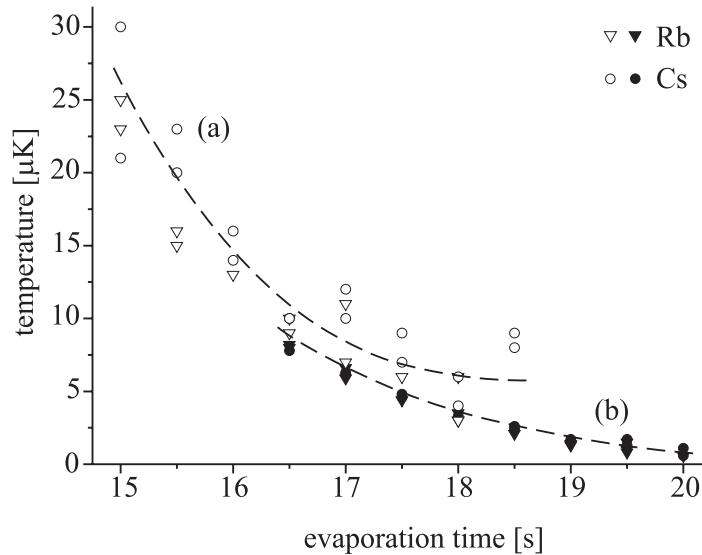


Figure 3. Two data sets from different experimental runs showing sympathetic cooling of Cs (\circ and \bullet) by Rb (∇ and \blacktriangledown). In data set (a) (open symbols) the initial Cs atom number at 15 s is about 10^6 ; apparently sympathetic cooling stops after 18 s, where Rb and Cs atom numbers are nearly equal. In data set (b) (filled symbols) the initial atom number of Cs is about 2×10^5 at 16.5 s and sympathetic cooling proceeds down to temperatures below $1 \mu\text{K}$. The dashed curves are only to guide the eye.

and starting with a pure $|2, 2\rangle$ ensemble, we achieve BEC after 23 s of evaporation with about 1×10^5 atoms in a nearly pure condensate. After accomplishing BEC of Rb by microwave cooling we performed sympathetic cooling of Cs down to temperatures below $1 \mu\text{K}$ using the same frequency ramp as for Bose condensing Rb. Figure 3 shows two data sets obtained from two different experimental runs. In the case of data set (a) one can clearly see that the cooling process stops after 18 s. At 18.5 s Rb was almost completely evaporated. For the experimental run corresponding to data set (b) the Cs atom number was chosen to be a factor of 5 smaller and sympathetic cooling is efficient down to a temperature of 700 nK; we did not pursue cooling the mixture further because, due to strong Cs losses (see figure 4), the Cs atom number became too low to be detected with our current imaging system. Improving our sensitivity to the detection of smaller Cs atom numbers will allow us to cool the mixture further and eventually to create a small sample of ultracold Cs immersed in a Bose-condensed cloud of Rb. In a separate experiment we studied the Cs losses while storing Cs in the presence and absence of Rb at $2 \mu\text{K}$. We found the losses to be non-exponential in both cases. From the measurements we obtain loss rate coefficients that are comparable to the value reported in [23] for spin dipole relaxation of Cs in the $|4, 4\rangle$ state. The lowest temperature for which the Cs losses were studied in [23] was $7 \mu\text{K}$, while the lowest Cs temperature reported was $4 \mu\text{K}$. However, at the moment the estimated error of our results is large; thus we can only say that we do not have evidence for inelastic Rb–Cs collisions.

The sympathetic cooling data in figure 3 show that the Cs temperature closely follows the Rb temperature on the time-scale of the evaporation process; this indicates a very efficient interspecies thermalization. To analyse the sympathetic cooling quantitatively, we use the

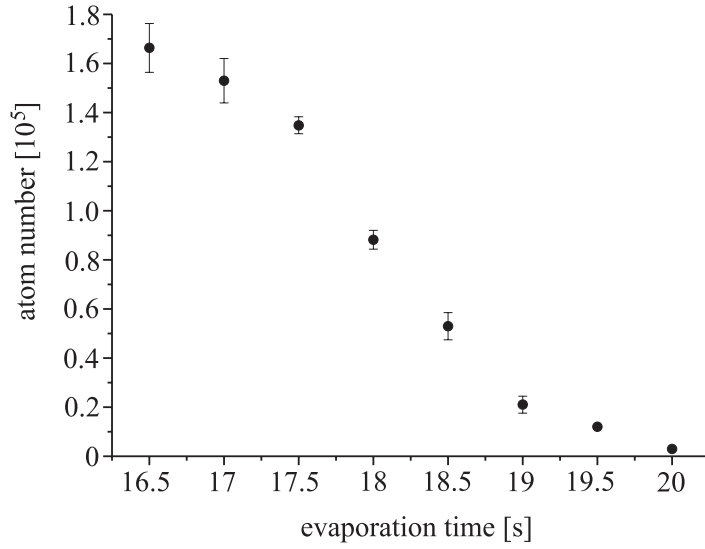


Figure 4. Cs atom numbers from data set (b) showing the strong losses after an evaporation time of 17.5 s, corresponding to a temperature of about $5 \mu\text{K}$.

following simple model. The Rb sample contains in the case of data set (a) at least twice as many atoms as the Cs sample, in the case of data set (b) at least ten times; we assume that under this condition the temperature evolution of the Rb cloud is determined by the evaporative cooling process only and not by the Cs temperature. The change in temperature of Cs is driven by thermal coupling to the Rb sample, i.e. elastic collisions, and the temperature difference between Cs and Rb. Quantitatively the thermal coupling is described by the thermalization rate Γ_{th} , which is the rate of elastic collisions Γ_{coll} divided by the number of collisions α needed for thermalization. We use a value of $\alpha = 2.7$, which was derived from Monte Carlo simulations [24] for the case of colliding atoms with equal mass. For different masses this number has to be divided by a kinematic factor $\xi = 4m_1m_2/(m_1 + m_2)^2$ [25]. The differential equation for Cs therefore is

$$\dot{T}_{\text{Cs}}(t) = -\Gamma_{\text{coll}}(t) \frac{\xi}{\alpha} (T_{\text{Cs}}(t) - T_{\text{Rb}}(t)). \quad (1)$$

The elastic collision rate is given by

$$\Gamma_{\text{coll}}(t) = \langle \sigma v_r \rangle_{\text{th}} \int d^3x n_{\text{Rb}}(\vec{x}, t) n_{\text{Cs}}(\vec{x}, t), \quad (2)$$

where $\langle \cdot \rangle_{\text{th}}$ denotes thermal averaging and v_r is the relative velocity of a Rb–Cs atom pair. The energy dependent elastic scattering cross-section to first order in k^2 [26] is

$$\sigma = \frac{4\pi a_{\text{RbCs}}^2}{k^2 a_{\text{RbCs}}^2 + 1}. \quad (3)$$

Thermal averaging of the energy dependent cross-section is performed extending the calculations presented in [27], section 2, to particles of different mass. We have integrated equation (1) numerically for several values of $|a_{\text{RbCs}}|$ and the results were compared to the measured Cs temperature evolution. Figure 5 shows some calculated temperature curves together with the measured values of both data sets (a) and (b).

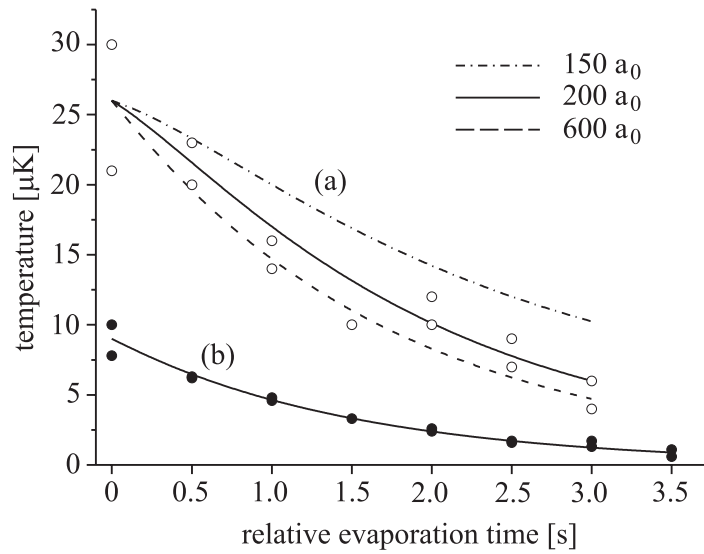


Figure 5. Comparison of the measured Cs temperatures from data sets (a) and (b) with the temperature evolution calculated with the model explained in the text. For this graph a common zero point on the time axis was chosen deliberately.

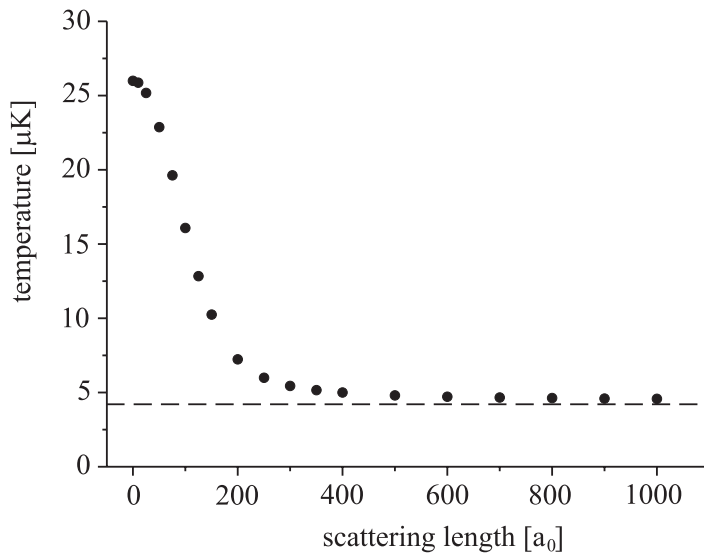


Figure 6. The calculated Cs temperature after 18 s of sympathetic cooling (see figure 3) as a function of the interspecies scattering length, calculated for data set (a) with the model described in the text. The dashed line represents the final Rb temperature.

For data set (a) values of the modulus of the scattering length larger than $200 a_0$ give temperature curves that describe the data well. For illustration, a significantly smaller value of $150 a_0$ and a large value of $600 a_0$ (which corresponds to the value given in [15]) were also included. As illustrated in figure 6, where the calculated final Cs temperature is plotted against the scattering length, the data cannot be used to discriminate scattering lengths above $\sim 250 a_0$.

Because of significantly higher Rb densities this holds even more in the case of data set (b), for which the calculated temperature curves are barely distinguishable and therefore only the result for $200 a_0$ is included in figure 5. Altogether we infer from the comparison of calculated temperature evolutions with measured temperatures a lower limit of $200 a_0$ for the modulus of the triplet *s*-wave scattering length of Rb and Cs.

A more exact method would be to cool Rb fast enough to decouple the temperature evolution of the Cs from the Rb, and observe the subsequent rethermalization. With our experimental conditions (densities and temperatures) we were not able to achieve such a decoupling of the Rb and Cs temperatures.

5. Conclusions and outlook

We have investigated sympathetic cooling of Cs by Rb that is evaporatively cooled with microwave radiation on the ground-state hyperfine transition. We find that the temperatures of Rb and Cs samples are strongly coupled and from the dynamics of the sympathetic cooling we estimate a lower limit for the modulus of the interspecies triplet *s*-wave scattering length of $200 a_0$. We have reached temperatures as low as 700 nK, which is the lowest temperature of Cs in the $|4, 4\rangle$ state reported to date. We were limited only by our present ability to detect Cs at atom numbers below a few thousand. We are confident that after improving our detection sensitivity and optimizing the evaporation ramp we will be able to create a small ultracold Cs sample inside a quantum degenerate Rb gas.

Acknowledgments

This work was supported by the Deutsche Forschungsgemeinschaft (Me971/22) within the Schwerpunkt ‘Ultracold quantum gases’. We thank C Marzok and C Zimmermann for valuable discussions and H Neff, W Hillert and C Grachtrup for help in the initial stages of the experiment.

Notes added. After submission of the paper an article was published by E Tiesinga, M Anderlini and E Arimondo [28], in which the authors present a refined analysis of the experimental results of [15, 16]. They give two possible values of the triplet scattering length of the Rb–Cs system: $700^{+700}_{-300} a_0$ and $(176 \pm 2) a_0$.

References

- [1] Truscott A G, Strecker K E, McAlexander W I, Partridge G B and Hulet R G 2001 *Science* **291** 2570
- [2] Schreck F, Khaykovich L, Corwin K L, Ferrari G, Bourdel T, Cubizolles J and Salomon C 2001 *Phys. Rev. Lett.* **87** 080403
- [3] Ospelkaus C, Ospelkaus S, Humbert L, Ernst P, Sengstock K and Bongs K 2006 *Phys. Rev. Lett.* **97** 120402
- [4] Papp S B and Wieman C E 2006 *Phys. Rev. Lett.* **97** 180404
- [5] Sage J M, Sainis S, Bergeman T and DeMille D 2005 *Phys. Rev. Lett.* **94** 203001
- [6] DeMille D 2002 *Phys. Rev. Lett.* **88** 067901
- [7] Chuu C-S, Schreck F, Meyrath T P, Hanssen J L, Price G N and Raizen M G 2005 *Phys. Rev. Lett.* **95** 260403
- [8] Klein A and Fleischhauer M 2005 *Phys. Rev. A* **71** 033605
- [9] Micheli A, Daley A J, Jaksch D and Zoller P 2004 *Phys. Rev. Lett.* **93** 140408

- [10] Daley A J, Fedichev P O and Zoller P 2004 *Phys. Rev. A* **69** 022306
- [11] Stan C A, Zwierlein M W, Schunck C H, Raupach S M F and Ketterle W 2004 *Phys. Rev. Lett.* **93** 143001
- [12] Ferrari G, Inguscio M, Jastrzebski W, Modugno G, Roati G and Simoni A 2002 *Phys. Rev. Lett.* **89** 053202
- [13] Goldwin J, Inouye S, Olsen M L, Newman B, DePaola B D and Jin D S 2004 *Phys. Rev. A* **70** 021601(R)
- [14] Jamieson M J, Sarbazi-Azad H, Ouerdane H, Jeung H, Lee Y S and Lee W C 2003 *J. Phys. B: At. Mol. Opt. Phys.* **36** 1085
- [15] Anderlini M, Courtade E, Christiani M, Cossart D, Ciampini D, Sias C, Morsch O and Arimondo E 2005 *Phys. Rev. A* **71** 061401(R)
- [16] Anderlini M, Ciampini D, Cossart D, Courtade E, Cristiani M, Sias C, Morsch O and Arimondo E 2005 *Phys. Rev. A* **72** 033408
- [17] Modugno G, Ferrari G, Roati G, Brecha R J, Simoni A and Inguscio M 2001 *Science* **294** 1320
- [18] Esslinger E, Bloch I and Hänsch T W 1998 *Phys. Rev. A* **58** R2664
- [19] Wohlleben W, Chevy F, Madison K and Dalibard J 2001 *Eur. Phys. J. D* **15** 237
- [20] Klempt C, van Zoest T, Henninger T, Topic O, Rasel E, Ertmer W and Arlt J 2006 *Phys. Rev. A* **73** 013410
- [21] Silber C, Günther S, Marzok C, Deh B, Courteille P W and Zimmermann C 2005 *Phys. Rev. Lett.* **95** 170408
- [22] Marzok C and Zimmermann C 2007 private communication
- [23] Söding J, Guéry-Odelin D, Desbiolles P, Ferrari G and Dalibard J 1998 *Phys. Rev. Lett.* **80** 1869
- [24] Wu H and Foot C J 1996 *J. Phys. B: At. Mol. Opt. Phys.* **29** L321
- [25] Mudrich M, Kraft S, Singer K, Grimm G, Mosk A and Weidemüller M 2002 *Phys. Rev. Lett.* **88** 253001
- [26] Joachain C J 1975 *Quantum Collision Theory* (Amsterdam: North-Holland)
- [27] Tol P J J, Hogervorst W and Vassen W 2004 *Phys. Rev. A* **70** 013404
- [28] Tiesinga E, Anderlini M and Arimondo E 2007 *Phys. Rev. A* **75** 022707

Corrigendum added 26 October 2007

Reanalysis of the experimental data has shown that the trapping frequencies of our magnetic QUIC trap as given in the manuscript have to be changed to $\omega_{\text{rad}} = 2\pi \cdot 190 \text{ Hz}$ and $\omega_{\text{ax}} = 2\pi \cdot 18 \text{ Hz}$. We have reanalyzed the numerical model for sympathetic cooling of Cs by Rb. Using the corrected values, figures 5 and 6 have to be replaced by figures 7 and 8, given below. From these we conclude a lower bound for the modulus of the Rb–Cs interspecies triplet *s*-wave scattering length of $150 a_0$. The other statements of the manuscript remain unchanged.

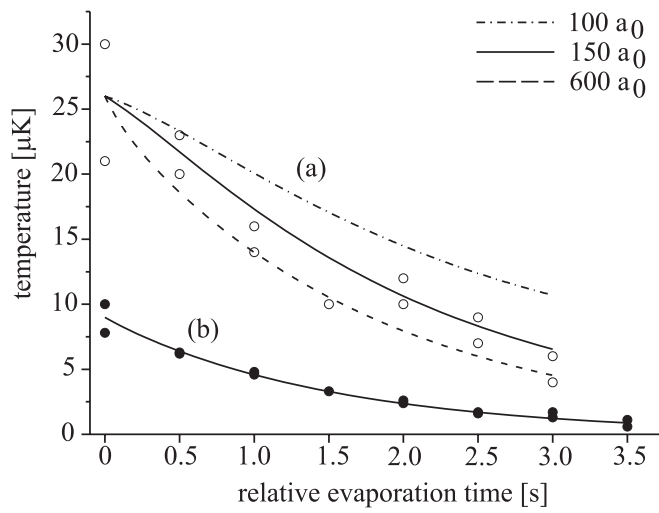


Figure 7. Comparison of the measured Cs temperatures from data sets (a) and (b) with the temperature evolution calculated with the model explained in the text. For this graph a common zero point on the time axis was chosen deliberately.

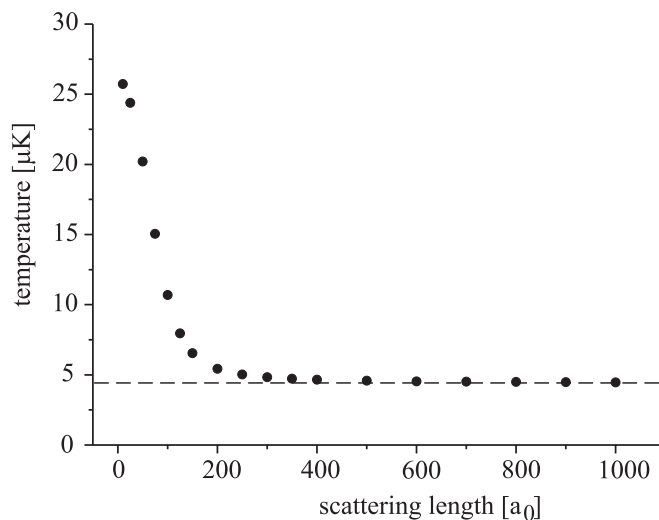


Figure 8. The calculated Cs temperature after 18 s of sympathetic cooling (see figure 3) as a function of the interspecies scattering length, calculated for data set (a) with the model described in the text. The dashed line represents the final Rb temperature.